Journal of Organometallic Chemistry 896 (2019) 77–82

Contents lists available at ScienceDirect

Journal of Organometallic Chemistry

journal homepage: www.elsevier.com/locate/jorganchem

Halogen bridged mixed-metal complexes based on a trimethylplatinum fragment

I.V. Skabitsky [a, *], E.I. Romadina [b, c], S.G. Sakharov [a], A.A. Pasynsky [a]

[a] Kurnakov Institute of General and Inorganic Chemistry, Russian Academy of Sciences, Leninskii pr. 31, Moscow, 119991, Russia
[b] Skolkovo Institute of Science and Technology, Nobel St. 3, Moscow, 143026, Russian Federation
[c] Institute for Problems of Chemical Physics, Russian Academy of Sciences, Semenov Prospect 1, Chernogolovka, Moscow region, 142432, Russian Federation

ARTICLE INFO

Article history:
Received 1 April 2019
Received in revised form
6 May 2019
Accepted 9 May 2019
Available online 20 May 2019

Keywords:
Trimethylplatinum
Rhodium
Ruthenium
Bridging chloride
Mixed-metal complex

ABSTRACT

By the reaction of tetramer $[Me_3Pt(\mu_3\text{-}Cl)]_4$ with $RhCl_3$ and [PPN]Cl (PPN = $Ph_3P=N=PPh_3^+$) in a acetone-DCM mixture under the influence of ultrasound a heterometallic ionic complex $[PPN][Me_3Pt(\mu\text{-}Cl)_3Rh(\mu\text{-}Cl)_3PtMe_3]$ (**I**) have been prepared. Tetranuclear complex $[PPN]_2$ $[(Me_3Pt)_2Ru_2(\mu\text{-}O)(\mu\text{-}Cl)_6Cl_4]^{2-}$ (**II**) have been obtained in a small yield starting from $RuCl_3$ in similar conditions. Complex **II** has also been prepared purposefully in higher yield by the action of $Me_3Pt(Me_2CO)_3][PF_6]$ on $[PPN]_4[Ru_2OCl_{10}]$. Both complexes were characterized by elemental analysis, ^1H, ^{13}C, and ^{195}Pt NMR spectroscopy, and their structures were determined by single crystal X-ray diffraction.

1. Introduction

Interest in heterometallic complexes and clusters is determined by the synergistic effect of various metals in the catalyst molecule [1] and the production of highly homogeneous nano-sized mixed-metal compositions during thermolysis of such compounds [2], often showing better catalytic properties than similar compositions obtained by deposition from a mixture of salts [3–5]. Notably, nanoparticles of a platinum-rhodium alloy are active for the oxidation of ethanol in direct ethanol fuel cells [6], and platinum-ruthenium compounds are active in the reaction of oxygen reduction in fuel cells [7].

It is known that a trimethylplatinum fragment can be used to construct heterometallic complexes by forming a direct Pt-Metal bond as in $BipyPtMe_3Mn(CO)_5$ (Bipy = 2,2′-bipyridine) [8] and $BipyPtMe_3ReO_3$ [9] or by the coordination of various metal containing ligands. By this way a great number of complexes were obtained, for example: the platinum-iridium and platinum ruthenium complexes $Cp^*Ir(C_3H_3N_2)_3PtMe_3$, $CymRu(C_3H_3N_2)_3PtMe_3$ [10] with pyrazolate bridges; rhenium-platinum hydroxide bridged cubanes [11]; sulfide bridged complexes $TpWS_3PtMe_3$ [12] and $Re_2((Me_3Si)_2C_2S_2)_2(S)_4(PtMe_3)_2$ [13]; phosphite bridged $CpCo((RO)_2PO)_3PtMe_3$ (R = Me [14], Et [15]) and tripple-decker complex $CpCo(C_3B_2Me_5)PtMe_3$ [16].

On the other hand, a lot of trinuclear homometallic complexes $[L_3M(\mu\text{-}X)_3M'(\mu\text{-}X)_3ML_3]^{n-}$ (X = Cl or I; M = M' = Ti [17],V [18],Mo [19],Re [20], Ru [21],Ni [22],Cu [23], Cd [24]) were structurally characterized, and two analogous mixed metal structures with Ir···Ag···Ir [25] and Ru···Rh···Ru [26] chloride bridged chains are known.

In this work we report the synthesis and characterization of halogen-bridged mixed-metal derivatives of trimethylplatinum: $[PPN][Me_3Pt(\mu\text{-}Cl)_3Rh(\mu\text{-}Cl)_3PtMe_3]$ (**I**) analogous to known complexes with trimetallic chains, and $[PPN]_2[(Me_3Pt)_2Ru_2(\mu\text{-}O)(\mu\text{-}Cl)_6Cl_4]$ (**II**) – product of the coordination of two $PtMe_3$ fragments to Ru_2OCl_{10} tetraanion in unusual structure type.

2. Experimental

2.1. Materials and general methods

All reactions were performed in dry solvents under an argon atmosphere using standard Schlenk techniques. $[Me_3PtCl]_4$ [27] and $K_4Ru_2OCl_{10}$ [28] were prepared as previously reported. All other chemicals and solvents were obtained from a commercial

* Corresponding author.
E-mail address: skabitsky@igic.ras.ru (I.V. Skabitsky).

https://doi.org/10.1016/j.jorganchem.2019.05.008
0022-328X/

source and were used as received without further purification. Infrared spectra were recorded with FTIR spectrometer « Bruker Alpha» with Platinum ATR accessory. Elemental analyses were performed on a CHNS analyzer EA3000 «EuroVector». ^{1}H (300.13 MHz), ^{13}C (75.4 MHz), and ^{195}Pt (64.5 MHz) NMR spectra were recorded on a Bruker AV 300 spectrometer, all ^{1}H and ^{13}C{^{1}H} NMR spectra were referenced to carbons or residual protons present in deuterated solvent (CD_2Cl_2) with respect to TMS, ^{195}Pt NMR spectra were referenced to Na_2PtCl_6 in D_2O used as external standard. CD_2Cl_2 was used without additional purification.

2.2. Synthesis of [PPN](PtMe$_3$)$_2$RhCl$_6$.(*I*)

A suspension of $[Me_3PtCl]_4$ (100 mg, 0.091 mmol), [PPN]Cl (98 mg, 0.17 mmol) and $RhCl_3 \cdot 3H_2O$ (51 mg, 0.19 mmol) in acetone (10 ml) and DCM (4 ml) was treated in ultrasound bath at 40 °C for 3 h. Volatiles were removed in vacuo, and the red solid obtained was triturated with heptane and extracted with DCM (7 × 2 ml). The extract was evaporated to ¼ its initial volume at reduced pressure and kept at −25 °C overnight. Complex **I** was isolated as red crystals (yield 14 mg). An additional amount of complex **I** was obtained as a pink powder by further evaporation of mother liquor and the addition of hexanes. Total yield: 24 mg (11%).

^{1}H NMR (CD_2Cl_2, 298 K) δ: 1.32 (s, $^{2}J_{PtH}$ = 81.8 Hz, 18H, Pt(CH_3)$_3$), 7.48, 7.66 (m, 30H, PPN^{+}).

^{13}C{H}(DEPT-135) NMR (CD_2Cl_2, 298 K) δ: 4.03 (s, $^{1}J_{PtC}$ = 750 Hz, Pt(CH_3)$_3$), 129.5 (m, $^{2}J_{C\text{-}P}$ = 13 Hz, $^{2}J_{P\text{-}P}$ = 7 Hz, *o*-Ph), 132.2 (m. $^{3}J_{C\text{-}P}$ = 11 Hz, $^{2}J_{P\text{-}P}$ = 7 Hz, *m*-Ph), 133.6 (s, *p*-Ph).

^{195}Pt{H} NMR (CD_2Cl_2, 298 K) δ: 2269.7 ($^{2}J_{Pt\text{-}Rh}$ 7.6 Hz).

IR (ATR, cm^{-1}): 3059 w., 2978 w.br., 2896 m, 2805 w., 1585 w., 1573 w., 1482 w., 1432 w., 1381 s.br., 1330 m, 1304 m.br., 1266 m, 1224 s, 1183 m, 1159 w., 1112 s.br., 1025 w., 997 m, 922 w., 855 w.br., 742 m, 721 v.s., 688 v.s, 585 m, 527 v.s, 497 v.s., 449 m, 441 m.

Anal. Calculated for $C_{42}H_{48}C_{l6}NP_2Pt_2Rh$ (1334.6 g/mol): C 37.30; H 3.51; N 1.01. Found: C 37.80; H 3.63; N 1.05.

2.3. Synthesis of [PPN]$_2$[(PtMe$_3$)$_2$Ru$_2$OCl$_{10}$] (*II*)

A suspension of $K_4Ru_2OCl_{10}$ (181 mg, 0.25 mmol) and [PPN]Cl (570 mg, 1 ммоль) in 10% hydrochloric acid (20 ml) was stirred for three days. During this period the solution was almost discolored, and the homogenous orange precipitate formed, which was filtered, washed with 10% hydrochloric acid, water, and dried in air.

A part of resulting orange powder (270 mg, 0.1 mmol $[PPN]_4Ru_2OCl_{10}$) was dissolved in DCM (10 ml) and solution of $Me_3Pt(Me_2CO)_3PF_6$, prepared from $[Me_3PtI]_4$ (73 mg, 0.05 mmol) and $AgPF_6$ (0.2 mmol) in acetone (10 ml) was added. Volatiles were removed in vacuo; the residue was dissolved in DCM (5 ml) and layered with toluene. The resulting mixture of large brown-orange and pale yellow crystals was washed with chloroform (3 × 10 ml) to remove the last. The orange-brown crystals were washed with toluene (2 × 10 ml) and recrystallized from DCM-toluene mixture. Yield: 66 mg (31%).

^{1}H NMR (CD_2Cl_2, 297 K) δ: 1.44 (br.s, $^{2}J_{PtH}$ = 78.8 Hz, 18H, Pt(CH_3)$_3$), 7.49, 7.67 (m, 60H, PPN^{+}).

^{1}H NMR (CD_2Cl_2, 233 *K*) δ: 1.27 (s, $^{2}J_{PtH}$ = 77.5 Hz, 6H, Pt(CH_3)$_3$), 1.41 (s, $^{2}J_{PtH}$ = 78.6 Hz, 6H, Pt(CH_3)$_3$), 1.55 (s, $^{2}J_{PtH}$ = 80.4 Hz, 6H, Pt(CH_3)$_3$), 7.47, 7.64 (m, 60H, PPN^{+}).

^{13}C{H}(DEPT-135) NMR (CD_2Cl_2, 233 K) δ: 1.79 (s, $^{1}J_{PtC}$ = 737 Hz, Pt(CH_3)$_3$), 0.99 (s, $^{1}J_{PtC}$ = 744 Hz, Pt(CH_3)$_3$), 1.46 (s, $^{1}J_{PtC}$ = 750 Hz, Pt(CH_3)$_3$), 129.2 (m, $^{2}J_{C\text{-}P}$ = 13 Hz, $^{2}J_{P\text{-}P}$ = 7 Hz, *o*-Ph), 131.7 (m. $^{3}J_{C\text{-}P}$ = 11 Hz, $^{2}J_{P\text{-}P}$ = 7 Hz, *m*-Ph), 133.4 (s, *p*-Ph).

^{195}Pt{H} NMR (CD_2Cl_2, 233 K) δ: 2212.3.

IR (ATR, cm^{-1}): 3058 (w,br), 2962 (w,br), 2892 (w,br), 2806 (w), 1586 (w), 1480 (w), 1435 (m), 1285 (m), 1268 (m), 1225 (m,br), 1183 (m), 1161 (w), 1111 (s,br), 1024 (w), 996 (m), 802 (w), 745 (m), 720 (vs), 689 (vs,br), 615 (w), 545 (s), 532 (vs,br), 497 (vs,br), 453 (m), 439 (m), 410 (w).

Anal. Calculated for $C_{72}H_{60}Cl_{10}N_2OP_4Ru_2$ (1649.8 g/mol): C 52.42; H 3.67; N 1.70. Found: C 52.74; H 3.65; N 1.85.

2.4. X-ray crystal structure determinations

The X-ray diffraction data of complexes **I** and **II** were collected on a Bruker SMART Apex II CCD diffractometer equipped with graphite-monochromated Mo (Kα radiation λ = 0.71073 Å). Crystallographic data and structure refinement details for structures **I** and **II** are listed in Table 1. Absorption correction was applied using

Table 1
Data collection and refinement statistics for structures **I** and **II**.

Empirical formula	$C_{42}H_{48}Cl_6NP_2Pt_2Rh$	$C_{39}H_{39}Cl_5NO_{0.5}P_2PtRu$
Formula weight	1334.54	1065.06
Temperature/K	150	150
Crystal system	triclinic	triclinic
Space group	P-1	P-1
a/Å	9.2527(9)	12.5157(12)
b/Å	11.5666(12)	16.2013(16)
c/Å	12.0329(12)	20.909(2)
α/°	104.8800(14)	82.501(2)
β/°	96.8919(13)	74.7590(10)
γ/°	112.1181(13)	83.2950(10)
Volume/Å^3	1118.74(19)	4040.5(7)
Z	1	4
ρ_{calc}g/cm^3	1.981	1.751
μ/mm^{-1}	7.062	4.273
F(000)	640.0	2084.0
Crystal size/mm^3	0.22 × 0.14 × 0.12	0.46 × 0.17 × 0.07
Radiation	MoKα (λ = 0.71073)	MoKα (λ = 0.71073)
2Θ range for data collection/°	4.436 to 59.998	4.06 to 56.714
Index ranges	−13 ≤ h ≤ 13, −16 ≤ k ≤ 16, −16 ≤ l ≤ 16	−16 ≤ h ≤ 16, −21 ≤ k ≤ 21, −27 ≤ l ≤ 27
Reflections collected	13431	42147
Independent reflections	6482 [R_{int} = 0.0283, R_{sigma} = 0.0372]	19928 [R_{int} = 0.0319, R_{sigma} = 0.0485]
Data/restraints/parameters	6482/0/250	19928/87/984
Goodness-of-fit on F^2	1.041	1.015
Final R indexes [I ≥ 2σ (I)]	R_1 = 0.0202, wR_2 = 0.0516	R_1 = 0.0358, wR_2 = 0.0810
Final R indexes [all data]	R_1 = 0.0215, wR_2 = 0.0523	R_1 = 0.0537, wR_2 = 0.0891
Largest diff. peak/hole/e Å^{-3}	1.24/-0.92	1.96/-2.00

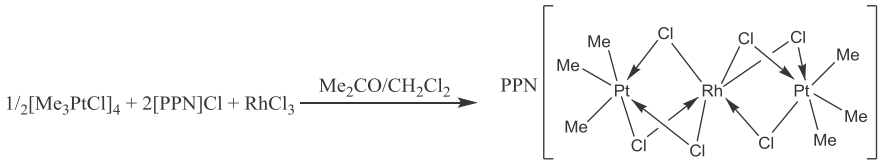

Scheme 1. Synthesis of compound **I**.

the SADAB program [29]. Using Olex2 [30], structures were solved with ShelXS program [31] by direct methods and refined with ShelXL [32] program using Least Squares refinement on F^2. All non-hydrogen atoms were refined anisotropically. Hydrogen atoms were positioned geometrically using a riding model with fixed isotropic thermal factors on carbon atoms.

2.5. Computational details

Theoretical calculations were carried out with the ORCA 4.1.1 program package [33]. A non-hybrid PBE functional [34], dispersion correction with Becke-Johnson damping (D3BJ) [35] and def2-TZVP basis set [36] with small-core pseudopotential for Ru and Pt atoms [37] were used for geometry optimization and Hessian calculation. Def2/J auxiliary basis [38] was used for Coulomb fitting. Single point energies were calculated on these geometries hybrid PBE0 functional [39] with the same basis sets and dispersion correction. The effect of solvent on single point energies in DCM were evaluated by SMD solvation model [40].

3. Results and discussion

3.1. Synthesis of rhodium-platinum complex *I*

The reaction of the cubane complex $[Me_3PtCl]_4$ with $RhCl_3 \cdot 3H_2O$ and [PPN]Cl (1: 2: 2 ratio) in a acetone-DCM mixture leads to the formation of the mixed-metal ionic complex [PPN] $[Me_3Pt(\mu\text{-}Cl)_3Rh(\mu\text{-}Cl)_3PtMe_3]$ (**I**) as red crystals insoluble in diethyl ether, hexanes and THF, upon recrystallization from DCM (yield 11%) (Scheme 1).

According to NMR spectral data, complex **I** is diamagnetic and all methyl groups are equivalent in solution. In the ^{1}H NMR spectrum of **I**, one signal of methyl groups on platinum was found at 1.32 ppm ($^2J_{PtH} = 81.8$ Hz), and one signal in the ^{13}C spectrum at −4.03 ppm, shifted upfield in comparison with reactant cubane complex (2.7 ppm) [41]. Notably, spin-spin coupling constant $^1J_{C\text{-}Pt}$ 750 Hz in 1 is almost unchanged with respect to the $^1J_{C\text{-}Pt}$ in $[Me_3PtCl]_4$ (746 Hz) despite the change in the coordination bridging type of ligands in trans position to methyl groups (μ^2-Cl, μ^3-Cl). The broad doublet in the ^{195}Pt spectrum at −2269 shows $^2J_{Pt\text{-}Rh}$ coupling of about 8 Hz, which may be compared with values of 27 and 6 Hz for $(C_5Me_5Rh)_2(\mu\text{-}CO)_2Pt(CO)(PPh_3)$ [42] and 24 Hz for thiolate bridged $[(PhCC)Pt(\mu\text{-}SCH_2Ph)(\mu\text{-}dppm)_2Rh(CO)][PF_6]$ [43].

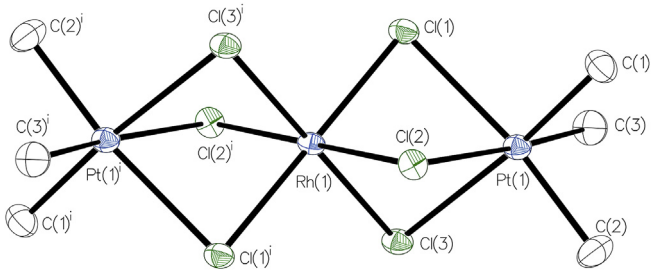

Fig. 1. The molecular structure of the anionic part of complex **I**. Hydrogen atoms are omitted for the sake of clarity. Selected bond lengths (Å) and angles (°): Pt(1) … Rh(1) 3.1414(3), Pt(1)–Cl(2) 2.5295(6), Pt(1)–Cl(1) 2.5370(6), Pt(1)–Cl(3) 2.5535(6), Pt(1)–C(1) 2.034(2), Pt(1)–C(2) 2.027(3), Pt(1)–C(3) 2.024(3), Rh(1)–Cl(1) 2.3497(6), Rh(1)–Cl(2) 2.3588(5), Rh(1)–Cl(3) 2.3538(6), Cl(1) … Cl(2) 3.2580(8), Cl(2) … Cl(3) 3.2430(8), Cl(1) … Cl(3) 3.2318(8), Rh(1)Cl(2)Pt(1) 79.89(2), Rh(1)Cl(1)Pt(1) 79.91(2), Rh(1)Cl(3)Pt(1) 79.489(2).

The structure of the complex **I** was determined by X-ray crystallography (Fig. 1). The distances between Rh and Pt 3.1414(3) Å are significantly larger than the sum of covalent radii of Pt and Rh (1.36 + 1.42 = 2.78 Å [44])) which corresponds with the absence of a metal-metal bond between d^6 Pt(IV) and Rh(III) ions. The bond distances Pt–Cl (2.5295(6) - 2.5535(6) Å) are slightly longer than the Pt–Cl distances in reactant cubane (2.489 Å [45]) and significantly longer than covalent radii sum (1.36 + 1.02 = 2.38 Å [34]) for both complexes, probably, due to the strong trans influence of methyl groups (Pt–C 2.024(3) - 2.034(2) Å). On the other hand, the bond distances Rh–Cl (2.3497(6) - 2.3588(5) Å) are shorter than covalent radii sum (1.42 + 1.02 = 2.44 Å [34]), but showed almost no difference with distances in free $RhCl_6^{3-}$ anion in salts with organic cations (2.321–2.377 [46,47]) and Rh–Cl distances in mixed-metal complex $[(PEt_3)_3Ru(\mu\text{-}Cl)_3Rh(\mu\text{-}Cl)_3Ru(PEt_3)_3]^+$ (2.339–2.341 Å) [26] of analogous structure.

3.2. Synthesis of ruthenium-platinum complex *II*

Attempt to perform a similar reaction with $RuCl_3$ instead of $RhCl_3$ resulted in the isolation of small amount of new mixed-metal

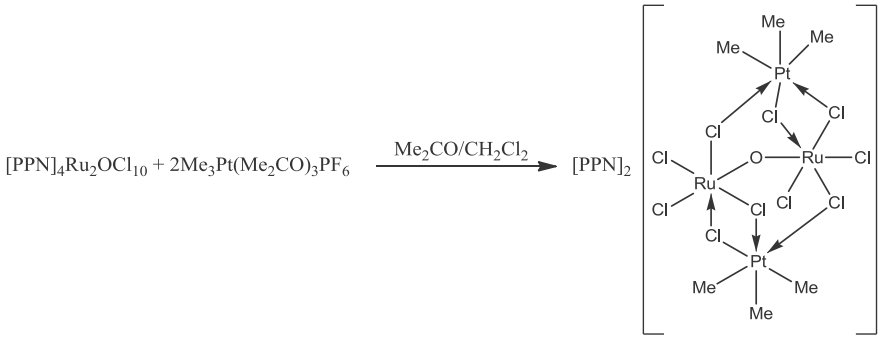

Scheme. 2. Synthesis of compound II.

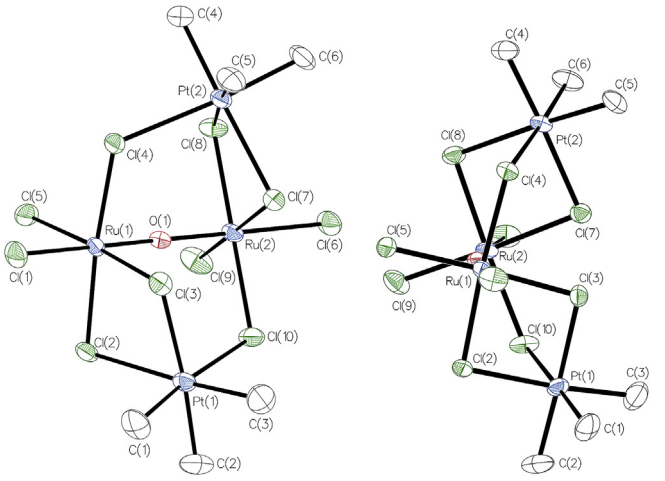

Fig. 2. The molecular structure of the anionic part of complex **II**. Hydrogen atoms are omitted for the sake of clarity. Selected bond lengths (Å) and angles (°): Pt(1)–C(1) 2.039(5), Pt(1)–C(2) 2.029(5), Pt(1)–C(3) 2.015(5), Pt(2)–C(4) 2.028(5), Pt(2)–C(5) 2.033(5), Pt(2)–C(6) 2.030(5), Pt(1)–Cl(3) 2.486(1), Pt(2)–Cl(7) 2.492(1), Pt(1)–Cl(2) 2.543(1), Pt(2)–Cl(8) 2.516(1), Pt(1)–Cl(10) 2.563(1), Pt(2)–Cl(4) 2.578(1), Ru(1)–Cl(3) 2.382(1), Ru(2)–Cl(7) 2.418(1), Ru(1)–Cl(2) 2.390(1), Ru(2)–Cl(8) 2.372(1), Ru(2)–Cl(10) 2.380(1), Ru(1)–Cl(4) 2.384(1), Ru(2)–Cl(9) 2.323(1), Ru(1)–Cl(5) 2.327(1), Ru(1)–Cl(1) 2.310(1), Ru(2)–Cl(6) 2.299(1), Ru(2)–O(1) 1.772(3), Ru(1)–O(1) 1.771(3), Ru(1)O(1)Ru(2) 168.8(2).

compound $[PPN]_2[Ru_2OCl_{10}(PtMe_3)_2]$ (**II**) as orange-brown crystals. Complex **II** was also prepared by reaction of $[PPN]_4Ru_2OCl_{10}$ with two equivalents of $Me_3Pt(Me_2CO)_3PF_6$ generated from $[Me_3PtI]_4$ and $AgPF_6$ in acetone, analogously to the preparation of tetrafluoroborate complex [48] (Scheme 2).

According to X-ray crystallography (Fig. 2), $PtMe_3$ fragments are coordinated to two chlorides on one of ruthenium atom (Pt–Cl 2.486(1)-2.543(1) Å) and one chloride on another ruthenium atom (Pt–Cl 2.563(1) и 2.578(1) Å). Shortest Pt–Cl distances correspond to bonds with chlorides in *trans*-position to axial chlorides not involved in bonding with platinum. As two chlorides in *syn*-conformation relative to Ru–Ru axis are bonded to different $PtMe_3$ fragments Ru–O–Ru angle 168.8(2) is deformed from linear in the free anion. The bond distances Ru–O (1.771(3) and 1.772(3) Å) are almost equivalent and close in value to distances in free anion $Ru_2OCl_{10}^{4-}$ (1.78–1.80 Å [49]).

Nonequivalence of methyl groups is observed in ^1H and ^{13}C spectra at low temperature. So, the broad singlet 1.44 ppm ($^2J_{Pt-H} = 78.8$ Hz), found at room temperature splits into three signals of equal intensity (1.27, 1.41 and 1.55 ppm; $^2J_{Pt-H}$ 77.5, 78.6 and 80.4 Hz, respectively) upon cooling to 223 K. Signals of methyl carbons in $^{13}C\{H\}$ spectra are observable only at low temperatures. As for compound **I**, ^{13}C methyl signals −1.79, −0.99 and 1.46 ppm are shifted upfield in comparison with 2.7 ppm for chloride bridged cubane. Spin-spin coupling constants $^1J_{C-Pt}$ are close to each other (737, 744 and 750 Hz) and to the value observed for $[Me_3PtCl]_4$ (746 Hz). Together, this suggests that asymmetric coordination of $PtMe_3$ fragments to Ru_2OCl_{10} fragment observed in the crystal structure is retained in solution.

Other possible isomers of complex **II** were studied using DFT calculation. Optimized geometries and relative enthalpies of complex **II** isomers and transition states are shown in Fig. 3. The isomer **2a** present in the crystal structure is also the most stable one. Two isomers of Cs symmetry: **2b** and **2c** have 3.41 and 3.68 kcal/mol higher enthalpy than **2a**. One Pt–Cl bond breaking is accompanied with a twist of $PtMe_3$ fragment in the corresponding transition states TSab and TSac (15.51 and 16.76 kcal/mol), which makes isomerization to **2b** and back to **2a** the most probable mechanism for methyl groups chemical exchange observed in ^1H NMR spectra at room temperature.

The coordination of $PtMe_3$ fragment to three chlorides on one ruthenium atom was evaluated to be much less favorable as corresponding isomer **2d** has 6.57 kcal/mol higher enthalpy. As Cl···Cl

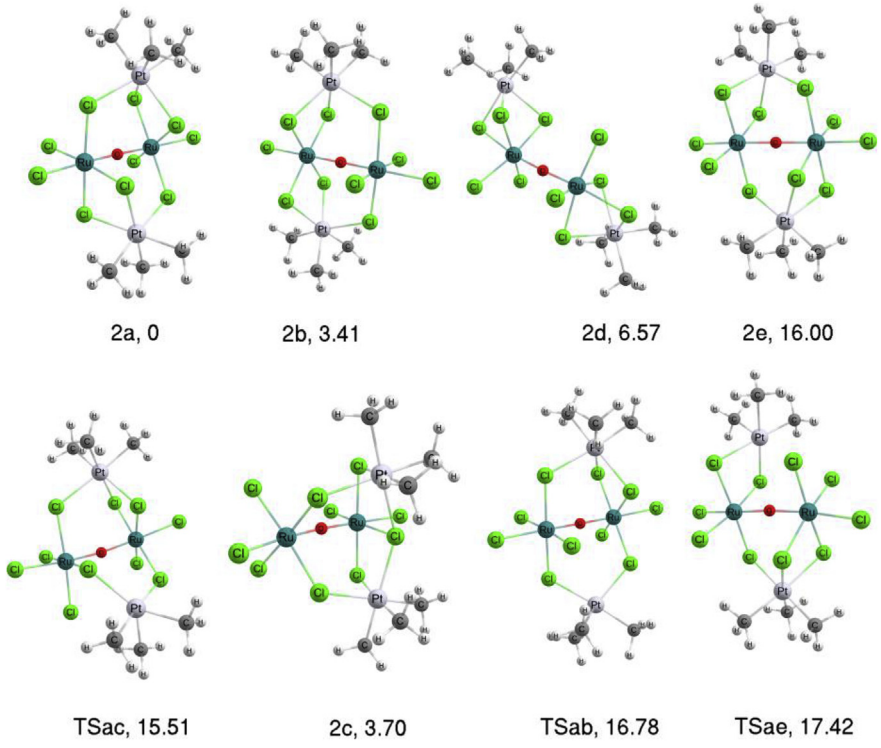

Fig. 3. Optimized geometries and relative enthalpies of dianion **II** isomers and corresponding transition states in DCM.

distances in **2e** (3.227, 3.231, 3.320 Å) are significantly shorter than.

Distances in **2a** (3.307, 3.662, 3.767 Å) and shorter than double Van der Waals radius of chlorine (3.716 Å) [50], apparently, 2e destabilization is due to steric repulsion between three chloride bridges, which also leads to more acute PtClRu angles about 81°. Notably, similar RhClPt angles were observed in the crystal structure of complex **I**, containing three chloride bridges binding every two metals.

The centrosymmetric isomer **2e** has prominently higher energy (16.00 kcal/mol), probably due to unavoidable deformation of the ligand environment of Pt and Ru from octahedral for this bonding pattern. Although corresponding transition state TSae is only slightly higher in energy (17.42 kcal/mol) than TSab, the enantiomerization process **2a** → TSae → **2e** → TSae → **2a** results in the exchange of only two of the three methyl groups.

4. Conclusions

In summary, the coordination of two cationic $PtMe_3$ fragments with octahedral anion $RhCl_6^{3-}$ and dimeric oxo-bridged $Ru_2OCl_{10}^{4-}$ was shown. In the latter case, unusual bonding pattern to chlorides on different ruthenium atoms was observed, accompanied by deformation of linear RuORu fragment. According to low-temperature NMR spectra asymmetric coordination of $PtMe_3$ fragments to Ru_2OCl_{10} fragment observed in the crystal structure is retained in solution.

Acknowledgements

This research was performed using the equipment of the JRC PMR IGIC RAS. This work was supported by the Russian Science Foundation (grant 18-73-10206).

Appendix A. Supplementary data

Supplementary data to this article can be found online at https://doi.org/10.1016/j.jorganchem.2019.05.008.

References

[1] P. Buchwalter, J. Rosé, P. Braunstein, Multimetallic catalysis based on heterometallic complexes and clusters, Chem. Rev. 115 (2015) 28–126.
[2] V.A. Grinberg, N.A. Mayorova, A.A. Pasynsky, A.A. Shiryaev, V.V. Vysotskii, I.P. Stolarov, I.A. Yakushev, N.V. Cherkashina, M.N. Vargaftik, Y.V. Zubavichus, A.L. Trigub, Nanosized catalysts of oxygen reduction reaction prepared on the base of bimetallic cluster compounds, Electrochim. Acta 299 (2019) 886–893.
[3] S. Zacchini, Using metal carbonyl clusters to develop a molecular approach towards metal nanoparticles, Eur. J. Inorg. Chem. 2011 (2011) 4125–4145.
[4] A.C.W. Koh, W.K. Leong, L. Chen, T.P. Ang, J. Lin, B.F.G. Johnson, T. Khimyak, Highly efficient ruthenium and ruthenium–platinum cluster-derived nanocatalysts for hydrogen production via ethanol steam reforming, Catal. Commun. 9 (2008) 170–175.
[5] E.R. Orskov, C. Fraser, The effects of processing of barley-based supplements on rumen pH, rate of digestion of voluntary intake of dried grass in sheep, Br. J. Nutr. 34 (1975) 493–500.
[6] M. Kim, C. Lee, S.M. Ko, J.-M. Nam, Metal alloy hybrid nanoparticles with enhanced catalytic activities in fuel cell applications, J. Solid State Chem. 270 (2019) 295–303.
[7] V.A. Grinberg, N.A. Maiorova, A.A. Pasynskii, V.V. Emets, A.A. Shiryaev, V.V. Vysotskii, V.K. Gerasimov, V.V. Matveev, E.A. Nizhnikovskii, V.N. Andreev, Nanostructured catalysts for direct electrooxidation of dimethyl ether based on Bi- and trimetallic Pt–Ru and Pt–Ru–Pd alloys prepared from coordination compounds, Russ. J. Coord. Chem. 43 (2017) 206–212.
[8] S. Komiya, S. Ezumi, N. Komine, M. Hirano, Organometallics 28 (2009) 3608–3610.
[9] K.R. Pichaandi, L. Kabalan, H. Amini, G. Zhang, H. Zhu, H.I. Kenttämaa, P.E. Fanwick, J.T. Miller, S. Kais, S.M. Nabavizadeh, M. Rashdi, M.M. Abu-Omar, Mechanism of me–Re bond addition to platinum(II) and dioxygen activation by the resulting Pt–Re bimetallic center, Inorg. Chem. 56 (2017) 2145–2152.
[10] R. Contreras, M. Valderrama, E.M. Orellana, D. Boys, D. Carmona*, L.A. Oro*, M.P. Lamata, J. Ferrer, Synthesis and characterization of heterodinuclear RuPt and IrPt complexes containing pyrazolate bridging ligands. Crystal structure of $[(\eta^5\text{-}C_5Me_5)Ir(\mu\text{-}pz)_3PtMe_3]$ (pz=pyrazolate), J. Organomet. Chem. 606 (2000) 197–202.
[11] U. Brand, C.A. Wright, J.R. Shapley, Synthesis and characterization of $\{Re(CO)_3\}^{4-}{}_n\{PtMe_3\}_n(OH)_4$, (n = 1–3). A set of heterobimetallic hydroxy cubane complexes, Inorg. Chem. 38 (1999) 5910–5912.
[12] H. Seino, N. Iwata, N. Kawarai, M. Hidai, Y. Mizobe, A series of dinuclear homo- and heterometallic complexes with two or three bridging sulfido ligands derived from the tungsten tris(sulfido) complex $[Et_4N][(Me_2Tp)WS_3]$ (Me_2Tp = hydridotris(3,5-dimethylpyrazol-1-yl)borate), Inorg. Chem. 42 (2003) 7387–7395.
[13] H. Seino, T. Kaneko, S. Fujii, M. Hidai, Y. Mizobe, Cubane-type heterometallic sulfido clusters: incorporation of two metal fragments into a dinuclear ReS(μ-S) 2 ReS core affording bimetallic M 2 Re 2 (μ 3 -S) 4 clusters (M = Ru, Pt, Cu) or trimetallic MM'Re 2 (μ 3 -S) 4 clusters via incomplete cubane-type MRe_2 (μ3 -S)(μ 2-S) 3 intermediates (M = Ru, Rh, Ir; M' = Mo, W, Pd, Ru, Rh), Inorg. Chem. 42 (2003) 4585–4596.
[14] R.E. Marsh, W.P. Schaefer, D.K. Lyon, J.A. Labinger, J.E. Bercaw, Structure of trimethylplatinum(IV) with a tripod ligand, Acta Crystallogr. Sect. C Cryst. Struct. Commun. 48 (1992) 1603–1606.
[15] R.E. Marsh, W.P. Schaefer, D.K. Lyon, J.A. Labinger, J.E. Bercaw, Structure of trimethylplatinum(IV) with a tripod ligand, Acta Crystallogr. Sect. C Cryst. Struct. Commun. 48 (1992) 1603–1606.
[16] A.S. Romanov, D.V. Muratov, P.V. Petrovskii, W. Siebert, A.R. Kudinov, The first triple-decker complex with the PtMe3 fragment: $CpCo(\mu\text{-}1,3\text{-}C_3B_2Me_5)PtMe_3$, Mendeleev Commun. 22 (2012) 13–14.
[17] L. Chen, F.A. Cotton, Synthesis, reactivity, and X-ray structures of face-sharing Ti(III) complexes; the new trinuclear ion, [Ti3Cl12]3–, Polyhedron 17 (1998) 3727–3734.
[18] K. Feghali, D.J. Harding, D. Reardon, S. Gambarotta, G. Yap, Q. Wang, Stability of Metal–Carbon bond versus metal reduction during ethylene polymerization promoted by a vanadium complex: the role of the aluminum cocatalyst, Organometallics 21 (2002) 968–976.
[19] J.C. Fettinger, J.C. Gordon, S.P. Mattamana, C.J. O'Connor, R. Poli, G. Salem, Anionic halomolybdate(III) chemistry. Tetrahydrofuran loss from $[MoX_3Y(THF)_2]^-$ (X, Y = Cl, Br, I), preparation and properties of $[Mo_3X_{12}]^{3-}$ (X = Br, I), and crystal structure of the edge-sharing trioctahedral $[PPh_4]_3[Mo_3I_{12}]$, Inorg. Chem. 35 (1996) 7404–7412.
[20] F. Calderazzo, F. Marchetti, R. Poli, D. Vitali, P.F. Zanazzi, Synthesis and crystal and molecular structures of mixed-valence tetranuclear, $[Re_4I_8(CO)_6]$, and trinuclear, $[Re_3I_6(CO)_6]$, compounds of rhenium obtained by di-iodine oxidation of rhenium(I) carbonyl complexes, J. Chem. Soc. Dalton Trans. (1982) 1665.
[21] A. Bino, F.A. Cotton, A linear, trinuclear, mixed-valence chloro complex of ruthenium, [Ru3Cl12]4-, J. Am. Chem. Soc. 102 (1980) 608–611.
[22] A. Gerdes, M.R. Bond, Octakis(dimethylammonium) hexa-μ2-chlorido-hexachloridotrinickelate(II) dichloride: a linear trinickel complex with asymmetric bridging, Acta Crystallogr. Sect. C Cryst. Struct. Commun. 65 (2009) m398–m400.
[23] A.V. Virovets, D.A. Piryazev, E.V. Lider, A.I. Smolentsev, S.F. Vasilevsky, L.G. Lavrenova, Specific non-valent iodine...chlorine interactions in the structures of copper(ii) chloride complexes with bis(3,5-dimethyl-4-iodopyrazol-1-yl)methane, J. Struct. Chem. 51 (2010) 92–98.
[24] C.E. Costin-Hogan, Chun-Long Chen, E. Hughes, A. Pickett, R. Valencia, N.P. Rath, A.M. Beatty, "Reverse" engineering: toward 0-D cadmium halide clusters, CrystEngComm 10 (2008) 1910.
[25] T.J. Morsing, K.P. Simonsen, J. Bendix, Outer sphere coordination chemistry: unusual six-coordinate silver(I) complexes with tri-halide–iridium(III) complexes as ligands, Inorg. Chem. Commun. 60 (2015) 61–64.
[26] M. Obies, N.R. Perkins, V. Arcisauskaite, G.A. Heath, A.J. Edwards, J.E. McGrady, Redox-dependent Metal–Metal bonding in trinuclear metal chains: probing the transition from covalent bonding to exchange coupling, Chem. Eur J. 24 (2018) 5309–5318.
[27] R.J.H. Clark, M.L. Franks, P.C. Turtle, Vibrational spectra, resonance Raman spectra, and electronic spectra of the.mu.-oxo-decachlorodiruthenium(IV) ion, J. Am. Chem. Soc. 99 (1977) 2473–2480.
[28] M. Atam, U. Müller, Die kristall- und molekularstruktur von trimethyl-platinazid, J. Organomet. Chem. 71 (1974) 435–441.
[29] G.M. Sheldrick, SADABS.//Göttingem, Univ. of Göttingem, Germany, 2005.
[30] O.V. Dolomanov, L.J. Bourhis, R.J. Gildea, J.A.K. Howard, H. Puschmann, OLEX2 : a complete structure solution, refinement and analysis program, J. Appl. Crystallogr. 42 (2009) 339–341.
[31] G.M. Sheldrick, A short history of SHELX, Acta Crystallographica Section A Foundations of Crystallography 64 (2008) 112–122.
[32] G.M. Sheldrick, Crystal structure refinement with SHELXL, Acta Crystallogr. C. Struct. Chem. 71 (2015) 3–8.
[33] F. Neese, Software update: the ORCA program system, version 4.0: software update, Wiley Interdisciplinary Reviews: Comput. Mol. Sci. 8 (2018) e1327.
[34] (a) J.P. Perdew, K. Burke, M. Ernzerhof, Generalized gradient approximation made simple, Phys. Rev. Lett. 77 (1996) 3865–3868;
(b) J.P. Perdew, K. Burke, M. Ernzerhof, Generalized gradient approximation made simple, Phys. Rev. Lett. 78 (1997), 1396–1396.
[35] (a) S. Grimme, S. Ehrlich, L. Goerigk, Effect of the damping function in dispersion corrected density functional theory, J. Comput. Chem. 32 (2011) 1456–1465;
(b) S. Grimme, J. Antony, S. Ehrlich, H. Krieg, A consistent and accurate ab

initio parametrization of density functional dispersion correction (DFT-D) for the 94 elements H-Pu, J. Chem. Phys. 132 (2010) 154104.
[36] F. Weigend, R. Ahlrichs, Balanced basis sets of split valence, triple zeta valence and quadruple zeta valence quality for H to Rn: design and assessment of accuracy, Phys. Chem. Chem. Phys. 7 (2005) 3297.
[37] D. Andrae, U. Haeussermann, M. Dolg, H. Stoll, H. Preuss, Energy-adjustedab initio pseudopotentials for the second and third row transition elements, Theor. Chim. Acta 77 (1990) 123–141.
[38] F. Weigend, Accurate Coulomb-fitting basis sets for H to Rn, Phys. Chem. Chem. Phys. 8 (2006) 1057.
[39] C. Adamo, V. Barone, Toward reliable density functional methods without adjustable parameters: the PBE0 model, J. Chem. Phys. 110 (1999) 6158–6170.
[40] A.V. Marenich, C.J. Cramer, D.G. Truhlar, Universal solvation model based on solute electron density and on a continuum model of the solvent defined by the bulk dielectric constant and atomic surface tensions, J. Phys. Chem. B 113 (2009) 6378–6396.
[41] T. Appleton, J. Hall, ^{1}H, ^{13}C and 195Pt n.m.r. spectra of Trimethylplatinum(IV) Tetramers $[PtMe_3Z]_4$: effects of Pt-Z-Pt and long-range Pt-Z-Pt-C couplings, Aust. J. Chem. 33 (1980) 2387.
[42] M. Green, R.M. Mills, G.N. Pain, F. Gordon, A. Stone, P. Woodward, Electrophilic behaviour of dicarbonylbis(pentamethylcyclopentadienyl)-dirhodium towards diazoalkanes and low-valent platinum compounds :X-Ray crystal structure of $[PtRh_2(\mu\text{-}CO)_2(CO)(PPh_3)(\mu\text{-}C_5Me_5)_2]$, J. Chem. Soc. Dalton Trans. (1982) 1309.
[43] A.L. Davis, R.J. Goodfellow, Multinuclear nuclear magnetic resonance studies of dirhodium and platinum-rhodium 'A-Frame' complexes of bis(dipheny1-phosphino)methane, J. Chem. Soc. Dalton Trans. (1993) 2273.
[44] B. Cordero, V. Gómez, A.E. Platero-Prats, M. Revés, J. Echeverría, E. Cremades, F. Barragán, S. Alvarez, Covalent radii revisited, Dalton Trans. (2008) 2832.
[45] R.E. Rundle, J.H. Sturdivant, The crystal structures of trimethylplatinum chloride and tetramethylplatinum, J. Am. Chem. Soc. 69 (1947) 1561–1567.
[46] W. Frank, G.J. Reiss, Spezielle, alkylammonium hexachlorometallates, II [1] synthesis, and crystal structure of bis(1,2-diammoniopropane) hexachlororhodate(III) chloride, $(H_3N\text{-}CH(CH_3)\text{-}CH_2\text{-}NH_3]\text{-}[RhCl_6]Cl$, Z. Naturforsch. B Chem. Sci. 51 (1996) 1459–1463.
[47] M. Bujak, W. Frank, Crystal structure of the inorganic-organic hybrid material tris(N,N′- dimethylethylenediammonium) bis(hexachloridorhodate(III)) dihydrate, $C_6H_{23}Cl_6N_3ORh$, Z. Kristallogr. N. Cryst. Struct. 229 (2014) 147–148.
[48] H. Junicke, C. Bruhn, D. Ströhl, R. Kluge, D. Steinborn, The first platinum(IV) complexes with glucopyranoside ligands, A New Coordination Mode of Carbohydrates, Inorganic Chemistry 37 (1998) 4603–4606.
[49] S.R. Nathan, N.W. Pino, D.M. Arduino, F. Perocchi, S.N. MacMillan, J.J. Wilson, Synthetic methods for the preparation of a functional analogue of Ru360, a potent inhibitor of mitochondrial calcium uptake, Inorg. Chem. 56 (2017) 3123–3126.
[50] J.K. Badenhoop, F. Weinhold, Natural steric analysis: ab initio van der Waals radii of atoms and ions, J. Chem. Phys. 107 (1997) 5422–5432.